

C. Giroud, S. Jachmich, P. Jacquet, A. Jarvinen, E. Lerche, F. Rimini,  
L. Aho-Mantila, I. Balboa, P. Belo, M. Beurskens, S. Brezinsek, I. Carvalho,  
F.J. Casson, I. Coffey, G. Cunningham, E. Delabie, S. Devaux, P. Drewelow,  
L. Frassinetti, A. Figueiredo, A. Huber, J. Hillesheim, L. Garzotti, M. Goniche,  
M. Groth, Hyun-Tae Kim, M. Leyland, P. Lomas, G. Maddison, S. Marsen,  
G. Matthews, A. Meigs, S. Menmuir, T. Puetterich, S. Saarelma, M. Stamp,  
A. Webster and JET EFDA contributors

# Towards Baseline Operation Integrating ITER-Relevant Core and Edge Plasma within the Constraint of the ITER-Like Wall at JET

“This document is intended for publication in the open literature. It is made available on the understanding that it may not be further circulated and extracts or references may not be published prior to publication of the original when applicable, or without the consent of the Publications Officer, EFDA, Culham Science Centre, Abingdon, Oxon, OX14 3DB, UK.”

“Enquiries about Copyright and reproduction should be addressed to the Publications Officer, EFDA, Culham Science Centre, Abingdon, Oxon, OX14 3DB, UK.”

The contents of this preprint and all other JET EFDA Preprints and Conference Papers are available to view online free at [www.iop.org/Jet](http://www.iop.org/Jet). This site has full search facilities and e-mail alert options. The diagrams contained within the PDFs on this site are hyperlinked from the year 1996 onwards.

# Towards Baseline Operation Integrating ITER-Relevant Core and Edge Plasma within the Constraint of the ITER-Like Wall at JET

C. Giroud<sup>1</sup>, S. Jachmich<sup>2</sup>, P. Jacquet<sup>1</sup>, A. Jarvinen<sup>3</sup>, E. Lerche<sup>2</sup>, F. Rimini<sup>1</sup>,  
L. Aho-Mantila<sup>4</sup>, I. Balboa<sup>1</sup>, P. Belo<sup>1</sup>, M. Beurskens<sup>1</sup>, S. Brezinsek<sup>5</sup>, I. Carvalho<sup>6</sup>,  
F.J. Casson<sup>1</sup>, I. Coffey<sup>7</sup>, G. Cunningham<sup>1</sup>, E. Delabie<sup>8</sup>, S. Devaux<sup>1</sup>, P. Drewelow<sup>9</sup>,  
L. Frassinetti<sup>10</sup>, A. Figueiredo<sup>6</sup>, A. Huber<sup>5</sup>, J. Hillesheim<sup>1</sup>, L. Garzotti<sup>1</sup>,  
M. Goniche<sup>11</sup>, M. Groth<sup>3</sup>, Hyun-Tae Kim<sup>1</sup>, M. Leyland<sup>12</sup>, P. Lomas<sup>1</sup>,  
G. Maddison<sup>1</sup>, S. Marsen<sup>10</sup>, G. Matthews<sup>1</sup>, A. Meigs<sup>1</sup>, S. Menmuir<sup>11</sup>, T. Puetterich<sup>6</sup>,  
S. Saarelma<sup>1</sup>, M. Stamp<sup>1</sup>, A. Webster<sup>1</sup> and JET EFDA contributors\*

*JET-EFDA, Culham Science Centre, OX14 3DB, Abingdon, UK*

<sup>1</sup>*EURATOM-CCFE Fusion Association, Culham Science Centre, OX14 3DB, Abingdon, OXON, UK*

<sup>2</sup>*ERM-KMS, Brussels Belgium*

<sup>3</sup>*Aalto University, Association EURATOM-Tekes, Otakaari 4, 02150 Espoo, Finland*

<sup>4</sup>*VTT Technical Research Centre of Finland, FI-02044 VTT, Finland*

<sup>5</sup>*EK-Plasmaphysik, Forschungszentrum Jülich, Association EURATOM-FZJ, Jülich, Germany*

<sup>6</sup>*Instituto de Plasmas e Fusão Nuclear, Instituto Superior Técnico, Universidade de Lisboa,  
1049-001 Lisboa, Portugal*

<sup>7</sup>*Astrophysics Research Centre, Queen's University, Belfast, BT7 INN, Northern Ireland, UK*

<sup>8</sup>*FOM-DIFFER, PO BOX 1207, 3430 BE Nieuwegein, The Netherlands*

<sup>9</sup>*Max-Planck-Institut für Plasmaphysik, Teilinstitut Greifswald, D-17491 Greifswald, Germany*

<sup>10</sup>*VR, Department of Physics, SCI, KTH, SE-10691 Stockholm, Sweden*

<sup>11</sup>*CEA, IRFM, F-13108 Saint-Paul-lez-Durance, France*

<sup>12</sup>*York Plasma Institute, Department of Physics, University of York, Heslington, York, YO10 5DD, UK*

\* See annex of F. Romanelli et al, "Overview of JET Results",  
(25th IAEA Fusion Energy Conference, St Petersburg, Russia (2014)).

Preprint of Paper to be submitted for publication in Proceedings of the  
25th IAEA Fusion Energy Conference, St Petersburg, Russia

13th October 2014 - 18th October 2014



## ABSTRACT

This paper reports experiments carried out at JET in the high-shape 2.5MA ELMy H-mode scenario to integrate the core plasma performance of ITER with an edge compatible with the metallic plasma facing component. Plasma with different divertor geometry are investigated with significant change in the pedestal density. Neon and nitrogen as a seed impurity are also compared with important difference in the pedestal pressure behaviour.

## 1. INTRODUCTION

The reference scenario for achieving  $Q=10$  in ITER is an integrated type-I ELMy H-mode scenario that combines good core plasma performance of  $H_{98(y,2)} \sim 1$ ,  $\beta_N \sim 1.8$ ,  $\langle n \rangle / n_{GW} \sim 0.85$ , and high fuel purity ( $Z_{\text{eff}} \sim 1.6$ ), together with edge parameters compatible with the Be/W Plasma Facing Components (PFCs) in stationary conditions for  $t_{\text{stat}} \sim 400\text{s}$  (i.e. 100 times the energy confinement time  $\tau_E$ ). With the help of extrinsic impurity radiation in the divertor, the power flowing through the separatrix can be reduced such that only 5% reaches the divertor target plate at which level both inner and outer legs are partially detached between ELMs. The ELM energy losses will be restricted to be less than 0.7MJ, which corresponds roughly to  $\Delta W_{\text{elm}} / W_{\text{ped}}$  below 1%. The pedestal is the key interface to achieving the challenging integration of plasma core performance and divertor compatibility with the metallic PFCs. ITER core requirements necessitates a high pedestal density and temperature. The ITER inductive scenario (with a plasma triangularly  $\delta \sim 0.4$ ) relies on the improved pedestal stability of high triangularity plasma for which the pedestal pressure is higher than in low  $\delta$  plasmas at a given pedestal density.

Previously, it was reported in JET that fuelled JET high- $\delta$  ELMy H-mode plasmas with  $I_p = 2.5\text{MA}$ ,  $B_T = 2.7\text{T}$ ,  $q_{95} \sim 3.3$ ,  $P_{\text{nb}} \sim 18\text{MW}$ , at high triangularity ( $\delta \sim 0.4$ ) had a pedestal pressure reduced by up to 40% with the change of PFCs from carbon (JET-C) to Be/W (JET-ILW) [1]. Plasma triangularity has no longer a beneficial effect on the pedestal pressure [2]. Discharges with similar pedestal density and different triangularity have a similar pedestal pressure. In these plasmas with horizontal target (HT) divertor geometry, N-seeding partially recovered the pedestal pressure loss [1]. The improvement of confinement at high- $\delta$  with respect to low- $\delta$  plasmas at a given pedestal density, and same divertor geometry, seems to have been re-established with nitrogen seeding [2]. Plasma performance, close the ITER requirements, was achieved but plasma conditions were not stationary ( $t_{\text{stat}} / \tau_E \sim 6$ ) due to the loss of sawtooth activity leading to W accumulation in the core.

Here new experiments are reported that identify the increase in pedestal pressure with N seeding to be depending on plasma triangularity and not specific to a plasma configuration. This paper shows how the operational space for the integrated scenario with nitrogen seeding has been expanded to: i) stationary plasma conditions ii) at lower  $n_{\text{ped}} / n_{\text{GW}}$  and iii) to plasmas with different divertor geometries. Neon seeding has also been investigated in view of the JET-DT campaign were N is prohibited as a seed impurity due to the production of Ammonia.

## 2. N-SEEDING AND PLASMA TRIANGULARITY EFFECT ON ENERGY CONFINEMENT

The high- $\delta$  baseline ELMy H-mode plasma in JET-C could maintain a high normalized confinement ( $H_{98} \sim 1$ ) at high Greenwald fraction  $\langle n_e \rangle / n_{GW}$ , unlike observations made on other devices [3]. Here we verify that the increase in pedestal pressure with N in JET-ILW is linked to plasma triangularity and not the high- $\delta$  HT configuration. The JET ELMy H-mode scenarios discussed in this paper have  $I_p = 2.5\text{MA}$ ,  $B_T = 2.7\text{T}$ ,  $q_{95} \sim 3.4$ ,  $P_{nbi} \sim 15\text{--}18\text{MW}$ ,  $P_{RF} \sim 0\text{--}4\text{MW}$  with  $\delta \sim 0.4$ . The confinement benefit of N-seeding has been extended to include plasmas with a vertical target (VT) divertor configuration closer to the ITER divertor geometry.

A specific experiment was conducted in VT plasmas with  $I_p = 2.5\text{MA}$ ,  $B_T = 2.7\text{T}$ ,  $q_{95} \sim 3.2$ , where the plasma triangularity was changed from low- $\delta \sim 0.22$  to high- $\delta \sim 0.36$  whilst keeping the vertical target divertor configuration unchanged as well as using the same heating, fuelling and seeding waveforms. Without N seeding an increase of the plasma triangularity raises the density, but does not improve the stored energy in VT plasmas, similarly to HT plasmas [2]. However, N seeding in low- $\delta$  VT plasma increases the stored energy by 15% whereas in high- $\delta$  VT plasmas, N seeding increases the stored energy by 40%, see Fig. 1. No reference exists for this configuration in JET-C. These results clearly established that in JET-ILW, the increase in confinement with N-seeding is dependent on the plasma triangularity and not plasma configuration.

## 3. OPERATIONAL SPACE OF N SEEDED PLASMA WITH THE JET-C COUNTERPART

The operation space of high- $\delta$  HT and VT plasmas are compared and put in context with their JET counterpart in terms of integrated plasma performance, see Fig. 2. In JET-C, the high- $\delta$  HT plasmas could reach partial detachment with deuterium fuelling only, with plasma performance  $H_{98(y,2)} \sim 0.95$ ,  $n_{e,ped}/n_{GW} \sim 0.9$ ,  $\beta_N \sim 1.9$ ,  $Z_{eff} \sim 1.7$  (Pulse No: 76678). The divertor conditions were achieved relying on a raised C radiation due to increased D sputtering. The ELM energy losses were unacceptably large of about 200kJ or 10% of pedestal stored energy. With N seeding (and intrinsic C), high- $\delta$  HT plasmas closer to the ELM energy losses requirement for integrated plasma performance were obtained in type-III ELM regime with values of  $H_{98(y,2)} \sim 0.86$ ,  $n_{e,ped}/n_{GW} \sim 0.68$ ,  $\beta_N \sim 1.54$ ,  $Z_{eff} \sim 2.3$  (Pulse No: 76687) and ELM energy losses about 70kJ or 1% of the stored pedestal energy.

In JET-ILW, the unseeded high- $\delta$  HT plasmas have reduced energy confinement in comparison to JET-C but with N injection, the energy confinement is partially recovered, see Fig. 2, and the ELM energy losses are increased from 90kJ (Pulse No: 82806) in the unseeded plasmas to 130kJ (Pulse No: 82810) in the seeded case. At the highest nitrogen seeding rate, a similar trajectory in  $n_{e,ped}/n_{GW}$  versus  $H_{98(y,2)}$  diagram to the one observed in N-seeded JET-C plasmas, the ELM energy losses is once again reduced to acceptable value of 70kJ. These plasmas are in type-III ELM regime with plasma performance are  $H_{98(y,2)} \sim 0.80$ ,  $n_{e,ped}/n_{GW} \sim 0.81$ ,  $\beta_N \sim 1.50$ ,  $Z_{eff} \sim 1.72$  (Pulse No: 82811). For the unseeded high- $\delta$  VT plasmas, the energy confinement is low  $H_{98(y,2)} \sim 0.6$  (Pulse No: 85262) with

similar ELM energy losses to the unseeded high- $\delta$  HT plasmas. As the N seeding rate is increased the normalized confinement is raised up to 0.85, (Pulse No: 85270) with ELM energy losses that reduced from 95kJ in unseeded case down to 54kJ in the seeded case.

The JET-C high- $\delta$  HT and JET-ILW high- $\delta$  HT and VT plasmas are compared in terms of their integrated plasma performance with as criteria a high density  $f_{GW} \sim 0.85$ , partially detached divertor and tolerable ELM energy losses (as a criteria  $\Delta W_{elm}/W_{ped} < 5\%$  is chosen in this paper as this is the detection limit of the stored energy measurement). Whether for the high- $\delta$  HT plasma in JET-C or in JET-ILW or the JET-ILW VT plasmas, the plasma performance are in fact fairly similar with  $H_{98(y,2)} \sim 0.86$ ,  $n_{e,ped}/n_{GW} \sim 0.6-0.76$ ,  $\beta_N \sim 1.5-1.6$ . Future experiments at JET will have to address whether the normalized confinement can be raised closer  $H_{98(y,2)} = 1$  and  $\beta_N \sim 1.8$  with higher input power whilst maintain small ELMs and partially detached divertor conditions.

#### 4. PEDESTAL HEIGHT OF JET-ILW N-SEEDED PLASMAS

The unexpected decrease in pedestal pressure for unseeded high shape plasmas has challenged our understanding of pedestal stability for high triangularity plasmas. The reduction in stored energy stems from a reduction in the pedestal pressure and mostly the pedestal temperature. It is still not know which mechanisms lead to low pedestal pressure in unseeded high- $\delta$  plasmas in JET-ILW with respect to JET-C, and what mechanism lead with N to an increase pedestal pressure in high- $\delta$  plasmas in JET-ILW. It still remains to be identified whether the effect is a result from the ion dilution in the pedestal region, or  $Z_{eff}$  or possible turbulence suppression. The current idea being investigated for the high- $\delta$  plasmas is that the pedestal structure and stability are affected by a change in fuel recycling and decrease in C content. An increase in the pedestal energy losses via charge-exchange processes seems unlikely, since EGDE2D-EIRENE simulations indicate that the order of magnitude of these losses is very small and the D0 flux crossing the separatrix is, in fact, predicted to increase with increasing divertor radiation in high- $\delta$  HT configuration [4].

Nitrogen seeding leads to an increase of energy confinement in both high- $\delta$  HT and VT plasmas and is due to an increase in pedestal pressure as shown in Fig.3 [1]. More information can be obtained with the identification of common features between the two configurations. For both high- $\delta$  HT and VT configurations the ELM-averaged pedestal pressure and temperature increase as a result of the seeding, see Fig.3. Opposite trends are observed for the pedestal density, which increases for high- $\delta$  HT plasmas whereas it decreases for the high- $\delta$  VT plasmas. In fact, plasmas with vertical target divertor geometry provide better control of the pedestal density than with a horizontal target configuration whilst maintaining the plasma performance of high- $\delta$  N seeded plasmas. It is likely that the difference in behaviour in electron pedestal density is linked to the difference in divertor geometry and its effect on neutral recycling [4].

The comparison of the pedestal characteristics of high- $\delta$  HT and VT N-seeded plasmas in the pre-ELM phase (Fig. 4) give further clue on change in pedestal stability with N seeding. In the HT plasmas the pre-ELM pressure still shows a strong increase with seeding. In contrast, the high- $\delta$  VT

pedestal pressure only show a small increase with N injection, unlike its ELM-averaged pedestal values, and not enough to explain the increase in global confinement. This difference is due to a reduction of the ELM energy losses with N seeding for high- $\delta$  VT plasmas. Nevertheless, the common feature between the seeded high- $\delta$  HT and VT is the increase in pedestal pressure due to an increase in pedestal temperature with respect to their respective unseeded reference plasmas. Interestingly, it is a reduction of the pedestal temperature that caused the drop in energy confinement in the high- $\delta$  plasmas with a change of PFCs. This rise of pedestal temperature with N seeding is most clear in the pre-ELM averaged pedestal data and any future mechanism proposed for the increase should be able to reproduce this trend.

## 5. OPERATIONAL SPACE, PEDESTAL HEIGHT OF NEON AND NITROGEN SEEDED HIGH- $\delta$ ELMY H-MODES

ITER plans to have the flexibility to use Ne, Ar and N<sub>2</sub> (or a mixture of) as seed gases, but it remains the case that chemically reactive species will be more of a safety challenge for the plant than a noble gas. In current devices, nitrogen plays the role that neon will have under ITER divertor conditions where the pedestal will be hotter  $\sim 3\text{--}4\text{keV}$  and its use in current machines also isolate the effect that high divertor radiation for power load reduction has on the integrated plasma performance.

At JET, Neon seeding experiments in ELMY H-mode have been carried out. As N is not compatible with future JET DT experiments, Ne will have to be the extrinsic radiator. Below an assessment of the difference in operational space between N and Ne for reaching partial detachment with stationary conditions is given. First, the difference in pedestal pressure with Ne and N seeding in high- $\delta$  ELMY H-mode is discussed which gives us further information on the pedestal stability of high- $\delta$  plasmas.

In JET-C, a comparative study on neon and nitrogen seeded high- $\delta$  HT plasma was carried out [5]. Both Ne and N could achieve a power load reduction at the outer target below  $1\text{MW}\cdot\text{m}^{-2}$  in the inter-ELM period with less than 10% decrease in the normalized energy confinement and in that respect both impurity were equivalent. There was however a difference in the localization of the radiation between the two species. When N was seeded, the main plasma radiative power,  $P_{\text{rad,main}}$ , was unaffected but the divertor radiative power,  $P_{\text{rad,div}}$ , was increased,  $P_{\text{rad,div}}/P_{\text{rad,main}}$  was increased to  $\sim 0.75$ . On the other hand, the value of this ratio was decreased as Neon was seeded ( $P_{\text{rad,div}}/P_{\text{rad,main}} \sim 0.45$ ) at the same fuelling rate. If the ratio  $P_{\text{rad,div}}/P_{\text{rad,main}}$  decrease as a result of impurity seeding, then as seeding is increase at best the pedestal conditions become non-stationary if close to a transition from type-I to type-III ELM regime and at worse the energy confinement is decreased due to a change of regime to type-III ELMY H-mode or L-mode. It was possible to reach with similar value of  $P_{\text{rad,div}}/P_{\text{rad,main}}$  with neon but at higher fuelling rate ( $4.3 \times 10^{22}\text{el/s}$ ) than for N seeded plasma ( $2.5 \times 10^{22}\text{el/s}$ ).

In JET-ILW, neon was seeded in high- $\delta$  VT plasmas with a similar input power and fuelling rate as their N-seeded counterpart. Motivated both by JET-C experience and results from EDGE2D

modelling [4], neon was not only seeded in high- $\delta$  VT plasma with the same D-fuelling ( $\Gamma_D \sim 2.5 \times 10^{22}$  el/s) and same input power ( $P_{\text{nbi}} \sim 15\text{--}19\text{MW}$ ,  $P_{\text{RF}} \sim 3\text{--}5\text{MW}$ ), but also with both a combination of higher NBI input power ( $P_{\text{nbi}} \sim 23\text{--}35\text{MW}$ ) at same fuelling rate ( $\Gamma_D \sim 2.5 \times 10^{22}$  el/s) and same input power at lower and higher D fuelling rate ( $\Gamma_D \sim 1.5 \times 10^{22}$  and  $4.5 \times 10^{22}$  el/s).

#### **4.1 PEDESTAL HEIGHT OF NEON VERSUS NITROGEN SEEDED DISCHARGES:**

The pre-ELM electron pedestal pressure, temperature and density as a function of neon seeding is shown in Fig.5. At all D-fuelling rates the pedestal pressure and density drop with increasing neon seeding rate unlike with nitrogen seeding. At the lowest and highest fuelling rate, the neon seeding rate was increased up to the level where L-mode phases appeared during the plasma duration. The pedestal conditions became nonstationary (as indicated on Fig.5). Even at the highest input power, the electron pedestal pressure is barely raised above 7kPa. The mechanism raising the pedestal temperature and thereby pressure with N seeding does not seem to take place with neon seeded plasma. In both the N and Ne seeded plasmas the effective charge,  $Z_{\text{eff}}$ , and dilution,  $n_D/n_e$ , was determined at the plasma edge region ( $0.6 < r/a < 0.8$ ) from the C, Be and Ne or N concentration measured with CXRS and High Resolution Thompson scattering. Figure 6 shows that a similar range of  $Z_{\text{eff}}$  and dilution and even normalized  $\beta_N$  is being probed with N and Ne seeded plasma with very different effect on the pedestal temperature. It is true that these values of  $Z_{\text{eff}}$  and dilution are measured at the pedestal top and not within the pedestal. Currently, methods are being developed to assess an improved  $Z_{\text{eff}}$  determination can be done within the pedestal with Bayesian technique using available continuum measurements. However, it is unlikely that the value of  $Z_{\text{eff}}$  or dilution differs significantly within the pedestal and are similar at the pedestal top ( $0.6 < r/a < 0.8$ ). Therefore, it appears unlikely that the  $Z_{\text{eff}}$  or dilution alone play a leading role in the increase in pedestal temperature and pressure for N seeded discharges.

#### **4.2 POWER LOAD REDUCTION AT OUTER TARGET OF NEON VERSUS NITROGEN SEEDED PLASMAS:**

The difference in operational space between Ne and N-seeded plasmas to access partially detached divertor with best plasma performance is discussed in terms of the ratio of the  $P_{\text{OT}}/P_{\text{net}}$  and  $P_{\text{rad,div}}/P_{\text{rad,main}}$ , with POT the power reaching the outer divertor estimated with Langmuir probe and the net power  $P_{\text{net}}$  ( $P_{\text{in}} - P_{\text{rad,main}}$ ).

N-seeded high- $\delta$  VT plasmas with divertor radiation of about 30% of  $P_{\text{net}}$  have a power reaching the outer target of about  $0.1 \times P_{\text{net}}$ , and are partially detached at the strike point [6]. Figure 7 illustrates that this value of  $P_{\text{OT}}/P_{\text{net}}$  cannot be easily achieved in Ne-seeded plasma with the same input power whether at the similar D-fuelling rate of  $2.5 \times 10^{22}$  el/s to the N-seeded plasmas or at higher D-fuelling rate of  $4.5 \times 10^{22}$  el/s. The lowest value of  $P_{\text{OT}}/P_{\text{net}}$  at each D-fuelling rate is limited by appearance of L-mode phases leading to non-stationary plasma conditions (see Fig 7), i.e.  $P_{\text{OT}}$  is increased due to a loss of energy confinement. Figure 8 also show that the ratio  $P_{\text{rad,div}}/P_{\text{rad,main}}$  is much reduced

in Ne-seeded plasma in comparison to N-seeded one, with as consequence non-stationary pedestal conditions as was expected from JET-C experience. At the highest input power only was it possible to reach with Neon seeding a similar value  $P_{OT}/P_{net}$  to the N-seeded plasmas and similar pedestal pressure to the unseeded reference plasmas. In other words, to reach partially detached divertor conditions similar to N seeded discharges and maintain a ELMy H-mode plasma, it is necessary to increase the input power with respect to the N seeded plasmas.

Nitrogen seeding provides a favourable situation for achieving integrated plasma performance were both an increased divertor radiation, increase pedestal pressure and low main plasma radiation ( $P_{rad,div}/P_{rad,main}$ ) can be achieved leading to a value of  $H_{98}$  value up to 0.85-0.9 with  $\beta_N \sim 1.6$ , see Fig.8. In contrast, with neon seeding, the pedestal pressure decreases and it is required to increase the input power to maintain the low pedestal pressure of unseeded plasmas. This results in a poorly performing plasma with  $H_{98(y,2)} \sim 0.65$  with  $\beta_N \sim 1.6$ . Finally, it is also made clear that at least for the given high- $\delta$  VT plasmas, it is necessary to have sufficient D fuelling to maintain a  $Z_{eff}$  below 2, see Fig 8. Although not shown here this also applies for N-seeded discharges.

## 6. ACHIEVING PLASMA STATIONARY CONDITIONS AND LONG PULSE DEMONSTRATION

The avoidance of W core accumulation in high- $\delta$  N-seeded plasma with VT or HT divertor configuration has successfully been improved by adding at least 3MW of central ICRH heating power [6,7]. More details on the mechanism and technique are given in [6]. Stationary plasma conditions were obtained for both N and Ne seeded plasmas, at a somewhat higher RF input power of 4–5MW for the latter. A demonstration of an integrated plasma performance with nitrogen seeding was carried out. Long pulse operation with N-seeding was achieved in the VT configuration (less restrictive energy limit) for at least 7s – where the duration was limited only by the available power, see Fig.9. It was possible to extend the plasma duration from  $t_{stat}/\tau_E \sim 3$  to 28. Integrated plasma performance close to the ITER performance were achieved at JET with Be/W PFCs. These stationary ELMy H-mode plasmas are a significant step towards the ITER requirements achieving  $H_{98(y,2)} \sim 0.85$ ,  $\beta_N \sim 1.6$ ,  $\langle n \rangle/n_{GW} \sim 0.85$ ,  $Z_{eff} \sim 1.6$ ,  $t_{stat}/\tau_E \sim 28$ ,  $\Delta W_{elm}/W_{ped} \sim 4\%$  with  $\Delta W_{elm} \sim 65\text{kJ}$  at 45Hz ( $f_{rad} \sim 0.55$ ) with very low divertor target power loading ( $< 3\text{MW.m}^{-2}$ ) and partial detachment between ELMs. Similar results have now been achieved with the JET-ILW [8].

In conclusion, progress has been made in how to integrate the ITER-relevant core and edge plasma within the constraints of an ITER-like wall in JET with its Be wall and W divertor. The increase pedestal pressure in JET-ILW with N-seeding is confirmed to be dependent on plasma triangularity and its effect is stronger for high- $\delta$  plasma (40%) than for low- $\delta$  plasmas (15%). The operational space for N-seeded scenario has been expanded to lower  $n_{ped}/n_{GW} \sim 0.45-0.6$  with plasmas with vertical divertor geometry whilst maintaining good normalised energy confinement of high- $\delta$  N-seeded plasmas with horizontal divertor geometry. Nitrogen seeding provides a favourable combined properties for integrated plasma performance as the divertor radiation can be increased

with minimised radiation in the main plasma and increased pedestal pressure. On the other hand, neon seeding is more challenging and as the divertor radiation is increased, the pedestal pressure decreases and the main plasma radiation increases. This narrows the operational space for neon seeded discharges to higher input power than N seeded discharges. Stationary N-seeded ELMy H-mode were obtained achieving plasma conditions of  $H_{98(y,2)} \sim 0.85$ ,  $\beta_N \sim 1.6$ ,  $\langle n \rangle / n_{GW} \sim 0.85$ ,  $Z_{eff} \sim 1.6$ ,  $f_{rad} \sim 0.55$ ,  $P_{RF} \sim 3\text{MW}$  with low divertor target power load and partial detachment between ELMs for 7s – an increase of  $t_{stat}/\tau_E$  from previous value of  $\sim 6$  to  $\sim 28$ . ITER inductive scenario is designed at a triangularity  $\delta \sim 0.4$  to benefit from the improved pedestal stability of high triangularity plasmas. Although it was recovered with N-seeding at JET, our understanding of the pedestal stability of high- $\delta$  plasmas has been challenged with the unexpected decrease in pedestal pressure with a change of plasma facing components and the identification of the mechanism at play has to be an area of active research.

### **ACKNOWLEDGEMENTS**

This work was supported by EURATOM and carried out within the framework of the European Fusion Development Agreement. The views and opinions expressed herein do not necessarily reflect those of the European Commission. This work was also part-funded by the RCUK Energy Programme under grant EP/1501045.

### **REFERENCES**

- [1]. Giroud, Nuclear Fusion 2013
- [2]. Beurskens, Plasma Physics and Controlled Fusion 2013
- [3]. IPB, 2007
- [4]. Jarvinen, IAEA14
- [5]. Giroud, Nuclear Fusion 2012
- [6]. Giroud, Plasma Physics and Controlled Fusion 2014
- [7]. Lerche, IAEA14
- [8]. Rapp, Nuclear Fusion 2009

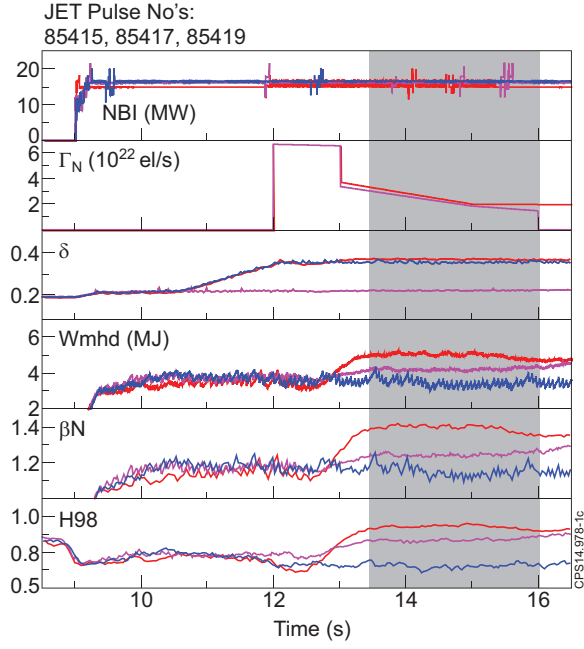


Figure 1 : Dependence of stored energy with plasma triangularity and N-seeding:

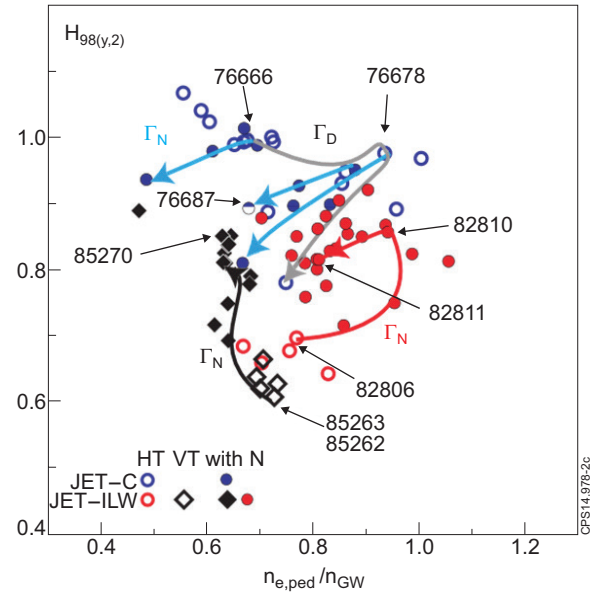


Figure 2:  $H_{98(y,2)}$  versus ratio of ELM-averaged electron pedestal density over Greenwald density for high- $\delta$  plasmas ( $f_G = n_{e,ped}/n_{GW}$ ). The lines and arrow indicate respectively in grey increase of D-fuelling in successive discharges in JET-C. The impact of N-seeding is indicated for JET-C in blue and leads to modest reduction in  $H_{98(y,2)}$  For JET-ILW in red (HT) and black(VT).

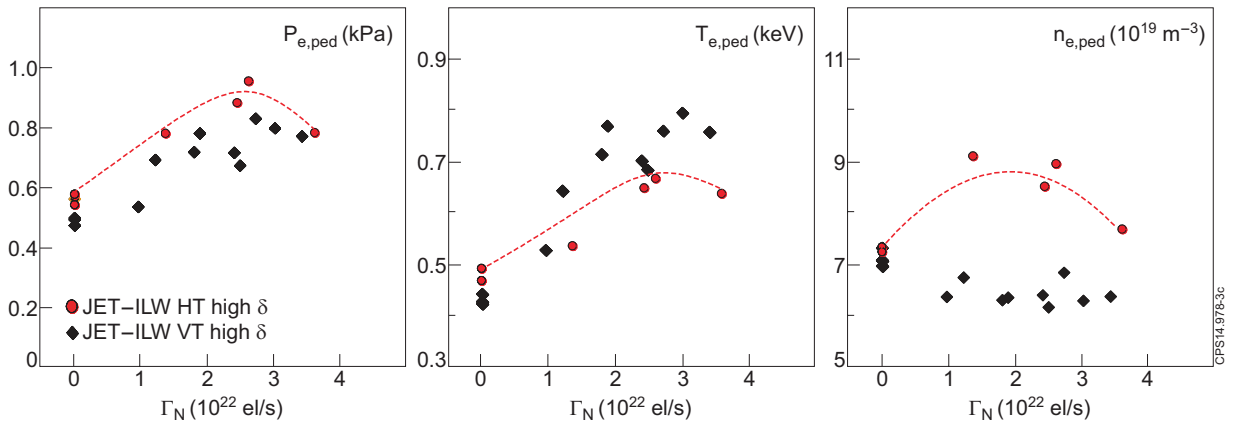


Figure 3: ELM-average pedestal electron temperature, density and pressure versus nitrogen seeding rate in high- $\delta$  HT and VT plasmas. Red circles correspond to high- $\delta$  HT plasmas. Black diamonds correspond to high- $\delta$  VT plasmas. N-seeded discharges are in filled symbols. Unseeded discharge in open symbols.

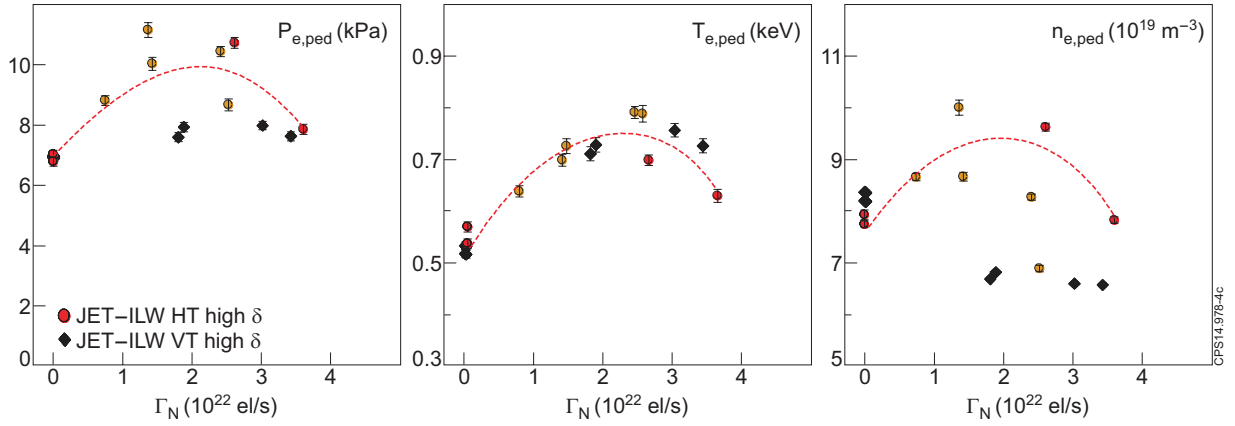


Figure 4: Pre-ELM pedestal pressure, temperature and density height in the time period 70 to 90% before an ELM as a function of the nitrogen seeding rate: Black diamond correspond to high- $d$  VT plasmas. Circles correspond to high- $\delta$  HT plasmas, red and yellow for fuelling rate greater and lower than  $2 \times 10^{22}$  el/s, respectively.

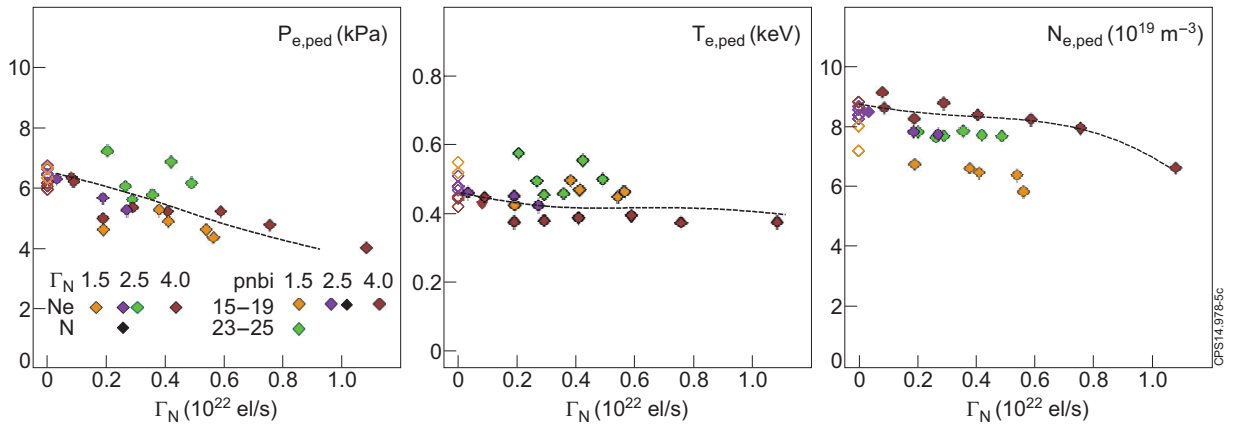


Figure 5: Height of electron pedestal pressure, temperature and density with increasing neon seeding rate in high- $\delta$ VT plasmas: Open and close symbol correspond to unseeded and seeded discharges respectively. Legends shown in Figure 6.

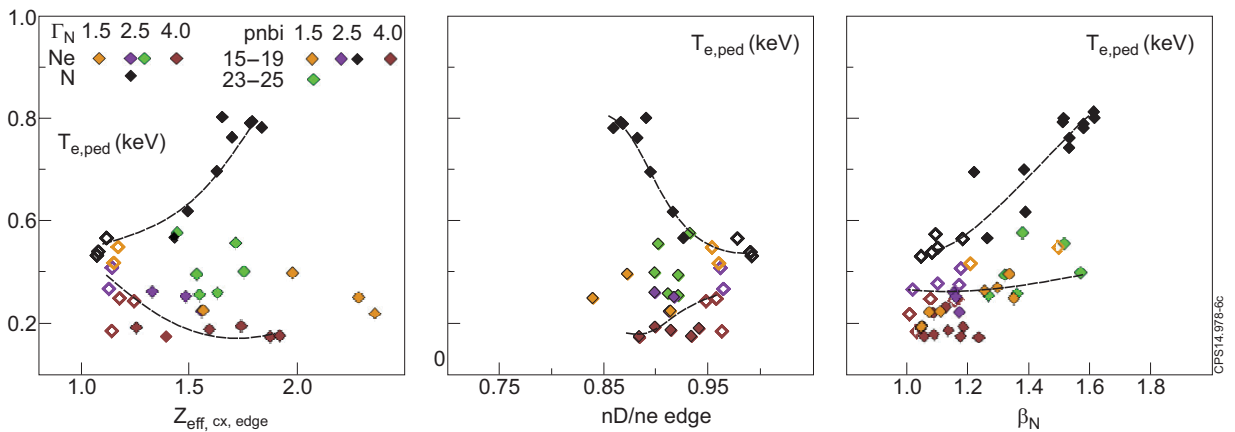


Figure 6: Pre-elm pedestal electron temperature versus  $Z_{eff,cx}$ , dilution and  $\beta_N$  for N and Ne seeded discharges.

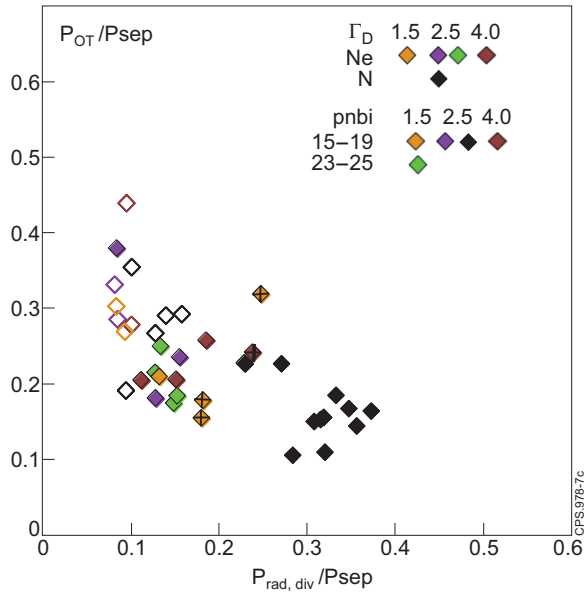


Figure 7: Ratio of power reaching the outer target over net power versus divertor radiative power over  $P_{net}$ .

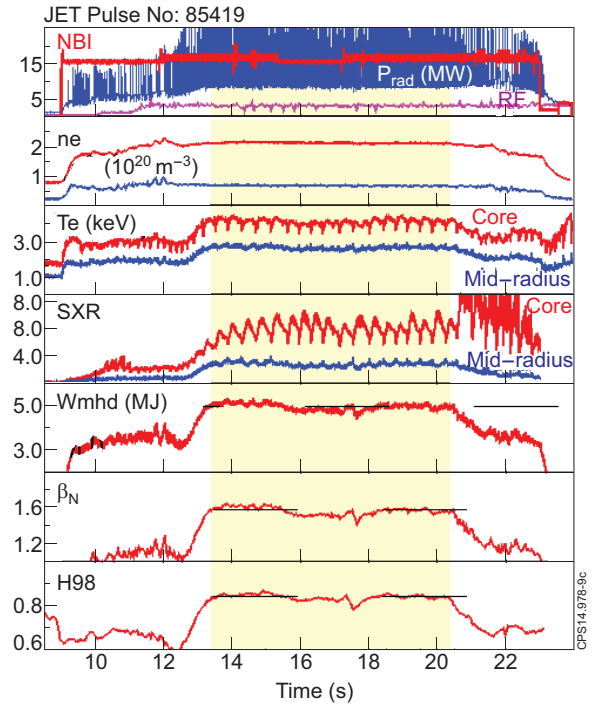


Figure 9: Time-trace for long  $N_2$ -seeded pulse number 85419 at radiation in the main plasma and increased pedestal 2.5MA/2.7T (VT).

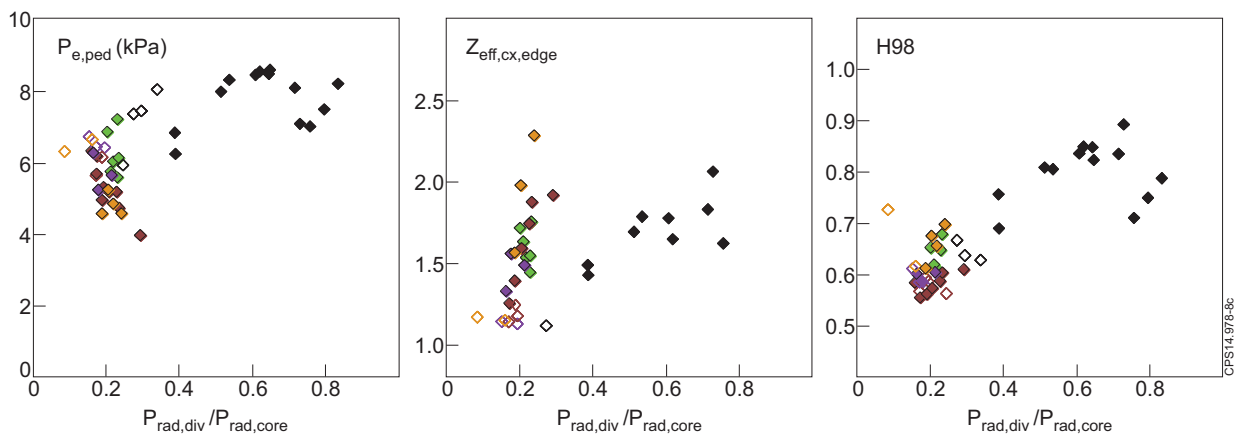


Figure 8: Pre-elm pedestal electron pressure,  $Z_{eff}$ ,  $H_{98}$  versus ratio of the divertor over main plasma radiative power.